Dielectric response of covered metal surfaces: Oxidation of Al(111)

M. Alducin
Departamento de Ingeniería Eléctrica, E.T.S. de Ingenieros Industriales y de Ingenieros de Telecomunicación, Universidad del País Vasco, Alda. de Urquijo s/n, E-48013 Bilbao, Spain

S. Peter Apell and I. Zoric
Department of Applied Physics, Chalmers University of Technology and Göteborg University, S-41296 Göteborg, Sweden

A. Arnau
Dpto. Física de materiales, Facultad de Química, Universidad del País Vasco, Apdo. 1072, 20080, San Sebastián, Spain
(Received 15 December 2000; revised manuscript received 10 April 2001; published 10 September 2001)

We have studied the response of an Al(111) surface at different stages of the oxidation process using a simple model for the dielectric response of the covered metal surface. Our model includes the metal response and the polarizability of the adsorbed oxygen atoms or oxide molecules depending on coverage. The experimentally measured surface plasmon energy shift to lower energies as the coverage increases is reproduced by our model and is consistent with STM observations that interpret the Al oxidation in two steps: first O atoms are adsorbed (up to coverages of the order of 0.5 monolayers) and then oxidation starts to take place.

DOI: 10.1103/PhysRevB.64.125410 PACS number(s): 73.90.+f, 78.20.Ci, 79.60.Dp, 81.65.Mq

I. INTRODUCTION

Since the first studies developed by Cabrera and Mott[1] in 1948, the oxidation of aluminum surfaces has been extensively studied in the last decades due to its scientific and technological interest.[2,3] However, there is still a certain controversy between the different theories and experimental data reported in the literature, which clearly indicates that the oxidation of metal surfaces on an atomic scale is still not fully understood.

The complexity of the problem, particularly at the early stages of the oxidation process, includes several steps that have been widely investigated by a variety of experimental techniques and theoretical models: adsorption of oxygen molecules and dissociation,[4–8] island formation,[4,9,10] difussion of the oxygen into the metal,[11–13] and last, nucleation and growth of the oxide compound.[1,14–16] There has been a special controversy regarding the existence or not of subsurface O absorption previous the oxide formation in the low coverage regime. Contrary to the early experiments which supported the existence of absorbed oxygen,[13] the more recent experiments[4,17] show no evidence for subsurface O absorption.

In an attempt to gain more insight we have studied, from a theoretical and experimental point of view, the first stages of the oxidation process by electron energy loss spectroscopy. Already in the early 1960's Powell and Swan[18] showed that EELS can be used to monitor the state of oxidation of Al and Mg foils from the shift of the low lying energy loss peak (associated with the surface plasmon excitation) and, therefore, confirmed the theoretical predictions of Stern and Ferrell.[19] These authors predicted a shift from the Ritchie's value $\omega_s = \omega_p/\sqrt{2}$ for the clean metal surface[20] to $\omega_s = \omega_p/\sqrt{1+\epsilon}$, where ϵ is the dielectric constant of the thick oxide layer. Our EELS data also show a clear shift of the surface plasmon loss peak to lower energies as oxygen coverage increases from clean Al surface up to a monolayer. The spectra measured at different coverages show a peculiar behavior: for coverages below 0.5 monolayers, the surface plasmon peak is slightly shifted to lower energies (about 0.5 eV), but at higher coverages the displacement rate increases sixfold (see Fig. 2). In order to explain this behavior we have modeled the surface response of an Al surface at different stages of the oxidation process using a dielectric formulation.[21] The dielectric function of the adlayer is constructed with the prescription of Bagchi *et al.*[22] based on the atomic polarizability of the adsorbed particles and their image dipoles on top of a simple metal surface. Our response function of the total system (metal + adlayer) shows that the observed change in the displacement rate of the surface plasmon peak can be ascribed to the beginning of the oxidation process. This result is in agreement with the pioneering interpretation of XPS data given by Bradshaw *et al.*[23] and, more recently, with the STM measurement reported by Brune *et al.*[4]

The outline of the paper is as follows. In Sec. II the experimental setup is described. The theoretical model is explained in Sec. III. Comparison and interpretation of our experimental and theoretical results are discussed in Sec. IV. Finally, a summary and conclusions of the present work are done in Sec. V.

II. EXPERIMENT

Measurements of plasmon energy change during oxidation of Al(111) were carried out in a conventional molecular beam scattering apparatus. An Al(111) crystal was mounted in the main scattering chamber (base pressure 1.10^{-10} Torr). Surface cleanliness was achieved by repeated cycles of sputtering and annealing until no oxygen or other impurities were observed in AES. Once a clean surface was established, oxygen was dosed to the surface via a conventional molecular beam line. A gold flag, positioned in front of the Al(111) crystal, enabled us to perform the sticking coefficient mea-

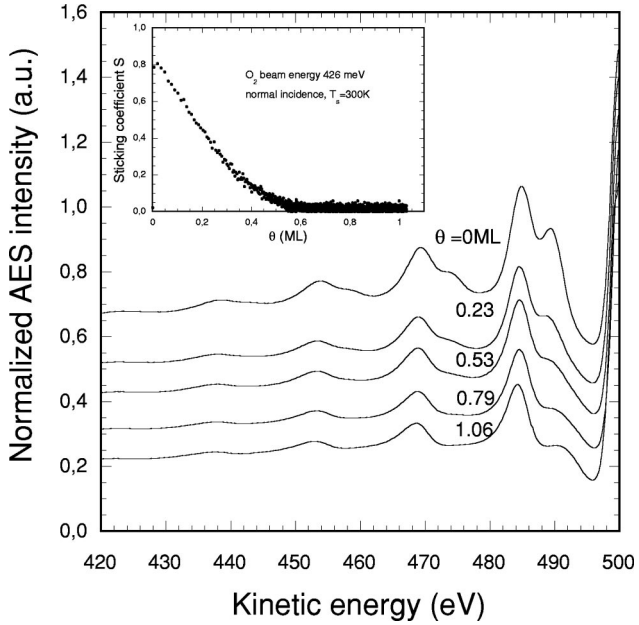

FIG. 1. Electron energy loss spectra, for inelastically scattered electrons from Al(111) surface, for a series of different oxygen coverages ranging from zero [clean Al(111) surface] to 1.06 ML (1 ML~1 oxygen atom/Al atom). The primary electron beam energy was 500 eV. The sample was at room temperature. The oxygen was dosed on the surface via a molecular beam at normal incidence. The inset in Fig. 1 shows the sticking versus coverage variation as obtained in a complete King and Wells run. The beam energy was 426 meV and the initial sticking coefficient was 0.8.

surements using a method of King and Wells.[24] Initially a complete King and Wells adsorption run was carried out yielding sticking coefficient and oxygen coverage versus exposure time. The absolute beam intensity, needed for absolute coverage determination, was obtained by shooting a beam directly into a stagnation detector.[25] The latter consists in a small stainless steel cell with a well-defined entrance aperture (known conductance) and a sensitive pressure gauge. The absolute beam intensity is related to the measured steady state pressure rise in the stagnation detector. In a subsequent series of runs, after the sample was cleaned and annealed, the adsorption process was divided into a discrete number of intervals, i.e., we carried out a series of *interrupted* King and Wells runs. After each interruption the oxygen coverage was determined from the ratio of areas under the O_2 partial pressure vs time curve for interrupted and complete King and Wells run. In this way a sequence of well-known oxygen coverages on the surface, varying from zero up to about one ML was established. Once the oxygen coverage was known, the sample was positioned in front of the Auger spectrometer, equipped with a single pass CMA, used for measurements of plasmon energy variations with oxygen coverage. The primary electron beam energy was 500 eV. In Fig. 1 we show the electron energy loss spectra, for inelastically scattered electrons from an Al(111) surface, for a series of different oxygen coverages, ranging from zero [clean Al(111) surface] to about one ML. The loss spectra reveal a series of bulk plasmon losses and several surface plasmon losses. We notice that the oxidation process does

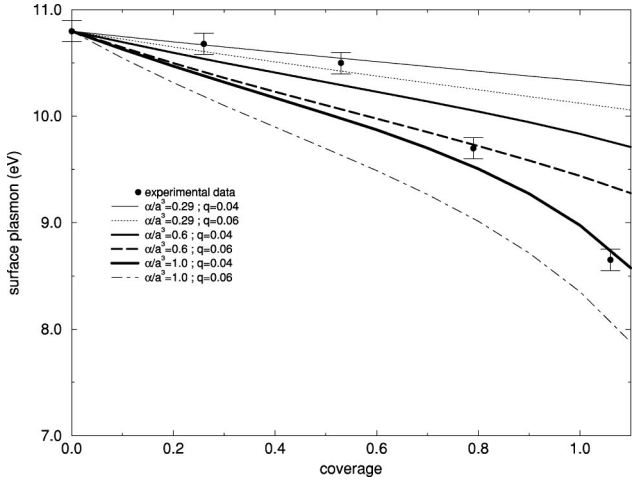

FIG. 2. Change in surface plasmon energy as a function of the oxygen coverage on the Al(111) surface. The black circles represents the experimental values obtained from the EELS spectra shown in Fig. 1. The asymptotic behaviour predicted by our theoretical model [see Eq. (8)] is shown for different values of the parallel momentum transfer q and the coupling constant κ (α/a^3), where α is the polarizability and a is the adsorbate radius. Comparison with the experimental data shows that the displacement of $\hbar\omega_s$ to lower energies cannot be accounted for only in terms of an increasing coverage keeping q and κ fixed.

not influence the bulk plasmon peak positions. In contrast, the surface plasmon energy is strongly influenced (shifted towards lower values) by the oxidation process. The results of our measurements for the surface plasmon energy variation vs oxygen coverage during the initial stage of Al(111) oxidation process are shown in Fig. 2 (black circles). In addition to the lowering of surface plasmon energy with increasing oxygen coverage we also observe a significant broadening of the electron loss peaks associated with surface plasmon creation events (see Fig. 1). This is consistent with appearance of a rather heterogeneous situation on the surface where, for a given total oxygen coverage, one has patches of clean surface, oxygen islands and 2D surface oxide present. All experiments are done at room temperature. A typical error in plasmon energy measurements is 0.1 eV. In the inset in Fig. 1 we also show the variation of the sticking coefficient versus O_2 coverage. In this case O_2 molecular beam ($E_k = 426$ meV) impinged at normal incidence on the sample. The high initial sticking coefficient (0.8) makes *interrupted* King and Wells type measurements easy to realize.

III. THEORY

The purpose of our theoretical model is to calculate a surface response function which characterizes the total system consisting of a metal substrate and a varying number of adsorbed particles on top of it. Let us consider an ordered two-dimensional array of adsorbed particles on top of a metal surface. Taking z as the coordinate perpendicular to the metal surface (defined as the image plane), the vacuum fills the half-space $z>0$ and the metal the half-space $z<0$. The adsorbed particles are located outside the metal at a distance

$z_0>0$ from the image plane and ordered parallel to the surface on a square array with unit length a_l. The dielectric response function to a longitudinal electric field, as is the case for EELS experiments, is the quasistatic limit ($c\to\infty$) of the reflection coefficient for incoming electromagnetic waves onto a metal surface.[26] Based on this equivalence, we use the theoretical reflection coefficient obtained in Ref. 21 for a system consisting of a film of thickness d and a semi-infinite substrate with dielectric function $\epsilon_b(\omega)$. The film may have two different dielectric functions depending on the direction of the applied electric field: $\epsilon_\parallel(\omega)$ for a field parallel to the metal surface and $\epsilon_\perp(\omega)$ for a perpendicular field. In the quasistatic limit and assuming $qd\ll 1$, the reflection coefficient of Ref. 21 for an incoming *p*-polarized EM wave reduces to

$$g(q,\omega)=\frac{\epsilon_b(\omega)-1+qd[\epsilon_\parallel(\omega)-\epsilon_b(\omega)/\epsilon_\perp(\omega)]}{\epsilon_b(\omega)+1+qd[\epsilon_\parallel(\omega)+\epsilon_b(\omega)/\epsilon_\perp(\omega)]}, \quad (1)$$

where q is the momentum transfer parallel to the surface. Notice that in the limit $d\to 0$, Eq. (1) reproduces the classical response function of a semi-infinite medium bound by vacuum.

In order to calculate the dielectric response function of a monolayer consisting of adsorbed particles, we describe each particle as an electric dipole with dipole moment $\mathbf{p}_i$. The effect of an external electric field on an adsorbed overlayer has been calculated using various formulations.[22,27,28] We use the one developed by Bagchi *et al.*[22] that obtains the dielectric response function of a dipolar monolayer by calculating the total electric field each particle feels. This field is the sum of two contributions: first, the field created by the rest of the dipoles forming the layer and second, the field due to the image dipoles induced at the metal surface. Since the image dipole is opposite to the direct one when parallel and equal when the dipole is perpendicular to the surface, the dielectric response function of the overlayer is different for parallel and perpendicular electric fields. The expressions derived within these assumptions are[22]

$$\epsilon_\parallel(\omega)-1=\frac{4\pi}{a_l^2 d}\,\frac{\alpha(\omega)}{1+\alpha(\omega)(\xi_0-\xi_I)/(2a_l^3)} \quad (2)$$

for an external electric field parallel to the metal surface and

$$1-\epsilon_\perp^{-1}(\omega)=\frac{4\pi}{a_l^2 d}\,\frac{\alpha(\omega)}{1-\alpha(\omega)(\xi_0+\xi_I)/(a_l^3)} \quad (3)$$

for an external electric field perpendicular to the metal surface. In these expressions, $\alpha(\omega)$ is the polarizability of the adsorbed particles, ξ_0 is a constant accounting for the electric dipolar field created by all the other particles, whereas ξ_I accounts for the electric field created by all the image dipoles. In particular, for a square layer, $\xi_0=-\Sigma(i^2+j^2)^{-3/2}=-9.0336\ldots$,[29] and

$$\xi_I=\frac{\epsilon_b(\omega)-1}{\epsilon_b(\omega)+1}\sum_{i,j=-\infty}^{\infty}\frac{3(2z_0/a_l)^2-[i^2+j^2+(2z_0/a_l)^2]}{[i^2+j^2+(2z_0/a_l)^2]^{5/2}}, \quad (4)$$

where $\epsilon_b(\omega)$ is the substrate (metal) dielectric function, as before.

The different adsorbed layers are characterized by different polarizabilities and different geometrical arrangements of the particles (a_l, d, and z_0). For simplicity, the particles are described as spheres of average radius a. Then, the thickness of the adsorbed layer is taken as $d=2a$, whereas the minimum value of the lattice parameter a_l is limited to $a_l\simeq 2a$. The theoretical model also imposes a restriction to the minimum value of z_0, the distance of each particle to the image plane, since the interaction between each particle (dipole) and its own image diverges when $z_0/a_l\ll 1$ [term $i=j=0$ in Eq. (4)]. Moreover, the reflection coefficient of Ref. 21 is obtained considering the film is on the substrate. Hence, the expression for the surface response function given in Eq. (1) is valid provided that $z_0<d$. Otherwise, the expression should be modified to include the z_0 dependence.

Inserting Eqs. (2) and (3) into Eq. (1) we can evaluate the surface dielectric function of the metal substrate with a varying number of adsorbates up to a monolayer. The different experimental coverages are modeled by taking different a_l values. More precisely, we define the coverage as $\theta=4a^2/a_l^2$. Hence, a compact monolayer ($a_l=2a$) corresponds to $\theta=1$ ML. For higher coverages, Eqs. (2) and (3) would have to be modified, so we limit our analysis for $\theta\leqslant 1$ ML.

In EELS experiments, in which the projectiles are electrons, the momentum transferred to the substrate is small enough to justify the use of a local response function $\epsilon_b(\omega)$. In the particular case of an Al substrate, $\epsilon_b(\omega)$ is well-described by a Drude dielectric function

$$\epsilon_b(\omega)=1-\frac{\omega_p^2}{\omega(\omega+i\gamma)} \quad (5)$$

with a bulk plasmon energy obtained from our EELS spectra, $\hbar\omega_p=15.6$ eV and damping $\hbar\gamma=1.37$ eV. Hence, the theoretical surface plasmon energy of a clean Al surface is $\hbar\omega_s=11.03$ eV.

IV. RESULTS

Figure 2 represents the surface plasmon energy of Aluminum as a function of the oxygen (O) coverage θ. The experimental data, plotted in black circles, show the shift of $\hbar\omega_s$ to lower energies as θ increases. It is remarkable the change around $\theta\simeq 0.5$ monolayer: for low coverages ($\theta<0.5$ ML), $\hbar\omega_s$ decreases at a rate $d(\hbar\omega_s)/d\theta\simeq 0.57$ eV/ML, whereas for $\theta>0.5$ ML the rate increases sixfold. For a clean Al surface ($\theta=0$ ML), the slightly different value of the experimental ω_s than the theoretical $\omega_s=\omega_p/\sqrt{2}$ is consistent with a negative surface plasmon dispersion for $qd_\perp\ll 1$, where $d_\perp$ is the centroid of the induced charge.[30] The equation for the q dependence of the surface plasmon frequency in the limit $qd_\perp\ll 1$ is

$$\omega_s(q)=\frac{\omega_p}{\sqrt{2}}\left(1-\frac{d_\perp q}{2}\right), \quad (6)$$

with $d_\perp$ evaluated at the frequency $\omega_p/\sqrt{2}$. Substitution of our experimental surface and bulk plasmon energies ($\hbar\omega_p = 15.6$ eV and $\hbar\omega_s = 10.8$ eV) in Eq. (6) gives us a good estimation of the parallel momentum transferred in the EELS experiments: $q \simeq 0.04$–0.05 a.u. ($d_\perp \simeq 0.8-1.2$ a.u. for a clean Al surface[30,31]). Since we are studying the surface but not the bulk plasmon energy, we use a Drude dielectric function with $\hbar\omega_p = 15.3$ eV [see Eq. (5)] to describe the q dependence of the Al surface response function that is not explicitly included in Eq. (1).

In view of these results, we have theoretically studied the dependence of the surface plasmon energy for different coverages with different parameters characterizing the adsorbed layer (α, z_0). We use static polarizabilities both for low and high coverages. The lack of structure of the EELS spectra around the surface plasmon energy loss suggests that the frequency dependence of the adsorbate polarizability is of minor importance. This is consistent with the fact that the thresholds in the excitation energy of the oxygen atom[32] and the aluminum oxide[33] are around 9 eV. Furthermore, at low coverages the probability of an electron to interact with an adsorbed oxygen is so small that no peaks are seen at the typical oxygen excitation energies in the EELS spectra.

An increase of the coverage, keeping fixed values of α and z_0, produces a shift of the surface plasmon peak to lower energies. This effect is also observed in metal substrates covered by a continuum dielectric film when increasing the film thickness d.[18,19] In our system the ω dependence of $g(q,\omega)$ is due to the metal substrate directly and indirectly through the image dipoles. To gain insight into the different contributions, we will first take $\xi_I = 0$. The surface plasmon frequency derived from Eq. (1) is then

$$\omega_s^2 = \frac{\omega_{s0}^2}{1 + (qd/2)[\epsilon_\parallel - (1/\epsilon_\perp)]}, \quad \text{for} \quad qd \ll 1, \tag{7}$$

where ω_{s0} is the surface plasmon frequency of the clean Al surface. As long as $\epsilon_\parallel$ and $\epsilon_\perp$ are greater than the vacuum value $\epsilon_0 = 1$, there will be a shift of ω_s to lower energies. From the definition of the coverage ($\theta = 4a^2/a_I^2$) and defining $\kappa = \alpha/a^3$, Eq. (7) can be rewritten as a function of coverage as

$$\omega_s^2 = \frac{\omega_{s0}^2}{1 + (\pi/4) qd\kappa\theta f(\theta)} \tag{8}$$

with

$$f(\theta) = \frac{1}{1 - \Delta\theta^{3/2}} + \frac{1}{1 + 2\Delta\theta^{3/2}}. \tag{9}$$

Notice that $\Delta = -(\xi_0\kappa)/16$ is a positive constant that depends only on the geometrical and electrical properties of the monolayer. For $\theta \ll 1$ ML, Eq. (8) reduces to $\omega_s/\omega_{s0} \simeq 1 - (\pi/4) qd\kappa\theta + O(\theta^2)$, but as the coverage approaches $\theta = \Delta^{-2/3}$, $f(\theta)$ begins to rule the asymptotic behavior which is then no longer linear.

The asymptotic dependence of ω_s on the coverage as predicted in Eq. (8) is plotted in Fig. 2 for different values either of the coupling constant $\kappa = 0.29, 0.6, 1.0$ or of the parallel momentum transfer $q = 0.04, 0.06$ a.u. We use $d = 5.2$ a.u. as a representative value for the layer thickness, that corresponds to take the neutral oxygen radius $a = 2.6$ a.u.[32] Comparing each curve to the experimental data represented in black circles, one observes that an increasing coverage cannot by its own reproduce the two slopes in the experimental data. Therefore, parallel to this it should be a change either of the polarizability or of the distance z_0, or both.

TABLE I. Average polarizabilities predicted by our theoretical model in order to reproduce the experimental displacement of the surface plasmon energy as coverage increases.

θ (ML)	0.26	0.53	0.79	1.0
$\hbar\omega_s$ (eV)	10.7	10.5	9.7	8.6
α (a_0^3)	5.4	5.9	15.4	18.5

As the adsorbates are closer to the surface, the contribution of the image dipoles to $\epsilon_\parallel(\omega)$ and $\epsilon_\perp(\omega)$ also produces a shift of ω_s to lower energies. However, a simple picture of the oxidation process in which the adsorbed oxygens are closer and closer to the surface as the coverage increases (i.e., z_0 varying from $2a$ to a) can only explain a change in the displacement rate of around 2–3 %, being far away from the experimental observations. Hence κ is the main parameter to affect the change of the surface plasmon frequency.

Keeping in mind the small influence of z_0, we take a fixed value $z_0 = 3$ a.u. and focus on the change in the polarizability per unit volume ($\kappa = \alpha/a^3$) as the number of adsorbed species increases. First, we consider the *low coverage* limit and assume that the adlayer is still made of oxygen atoms. Taking the oxygen atom polarizability $\alpha = 5.4$ a.u. and radius $a = 2.6$ a.u.,[32] which correspond to a coupling constant $\kappa = 0.29$, the theoretical displacement of ω_s for our experimental parallel momentum transfer $q = 0.04$ a.u. fits very well the measured data (see Fig. 2). We interpret this result as an indication of the importance of the screening by the few oxygen atoms present at low coverages.

As the coverage increases the reactive processes that are taking place between the substrate and the adsorbates cannot be mimicked in detail with our simple picture of a layer made of identical dipoles, since the adsorbed layer may consist both of neutral oxygen atoms and Al_2O_3. The complexity of the forming layer that goes through different stages: oxygen adsorption, island formation, and growth, and oxidation of the island edges, is observed in the STM experiments by Brune *et al.*[4] However, our model can provide us information of the heterogeneous adsorbates in terms of an average polarizability, i.e., we fix the adsorbate volume ($a = 2.6$ a.u.) and calculate the polarizabilities that fit the experimental data. The values that we obtain to reproduce the coverage dependence of the surface plasmon energy are shown in Table I. In principle we could use the oxygen polarizability and the alumina polarizability per unit volume to estimate from the experiments their proportions but for the present purposes we do not go into such a detailed treatment.

Up to half a monolayer the polarizability indicates that the adlayer is basically formed by oxygen atoms. However,

when 80% of the Al surface is covered, the polarizability is a factor 2.6 larger than that of oxygen. Finally, a slight increase of the polarizability is still needed to reproduce the surface plasmon energy at $\theta=1$ ML. This increase of α is in agreement with the beginning of the oxidation process in which the O and Al atoms start to form ionic molecular bonds, as mentioned above. We interpret the increase of α as a change in the charge state of the oxygen atom that is basically an O^{2-} anion in Al_2O_3. Other kind of contributions as structural changes (i.e., oxygen island formation and growth) are of minor importance. In this case, the increase of the polarizability would be accompanied by a corresponding increase of the volume of the adsorbate ($\sim$ number of O atoms in the island). Therefore, the coupling constant κ would remain almost similar to that of a single O atom.

It is remarkable that the same value $\hbar\omega_s(\theta=1\text{ML}) \simeq 8.7$ eV is obtained if we assume that the surface is completely oxidized and use the bulk dielectric function of Al_2O_3 (Ref. 33) to characterize the adsorbate dielectric functions $\epsilon\|(\omega)$ and $\epsilon_\perp(\omega)$ instead of Eqs. (2) and (3). Furtheremore, the experimental value $\hbar\omega_s=7.97$ eV at $\theta=1.32$ ML is in quite good agreement with the limit predicted by a dielectric continuum model ($\omega_s=\omega_p/\sqrt{1+\epsilon}$) (Ref. 19) applied to the particular case of an Al substrate covered with a very thick Al_2O_3 film, that is $\hbar\omega_s=7.8$ eV.

These theoretical results lead us to interpret our experimental data as follows: first, O atoms are adsorbed up to coverages of the order of 0.5 monolayers (and may be forming O islands) and only then some of the oxygens start to react with the Al atoms of the substrate giving rise to *new* adsorbates that are characterized by larger polarizabilities per unit volume. In other words, we can say that it is not enough to adsorb half a monolayer of oxygen to get half of the surface oxidized. Finally, the agreement between the experimental data and the dielectric continuum model at $\theta=1$ and 1.32 ML indicates that the surface is almost fully oxidized at $\theta=1$ ML.

V. CONCLUSION

The experimental data obtained from the EELS spectra show the displacement of the Al surface plasmon peak to lower energies when increasing the oxygen coverage up to a monolayer. There is a very clear change of the displacement rate at 0.5 monolayers that can be related to the oxidation process taking place at the Al surface.

Parallel to the experimental data, a theoretical model of the dielectric response function is proposed. In this model, the dielectric response function of a system consisting of a metal substrate with a finite number of adsorbates is derived as the quasistatic limit of the reflection coefficient of the corresponding system.[21] The Al substrate is represented by a Drude dielectric function, whereas the adsorbed layer is considered as a dipolar array above a metal surface.[22] In the limit of small momentum transfers ($qd \ll 1$), the dependence of ω_s on the coverage is obtained analytically. In principle, this behavior would explain a decrease of the plasmon energy with increasing coverage. However, we find that it is not possible to fit the experimental data unless a change of the adsorbate polarizability takes place with increasing coverage. Comparing our theoretical and experimental data, we conclude that the oxidation process might be described in two basic steps: first, neutral oxygen atoms are adsorbed on the Al surface up to a coverage of 0.5 monolayers and then the oxidation process starts to take place yielding a threefold increase of the adsorbate polarizability, when the oxygen goes from neutral to O^{2-} (the charge state in Al_2O_3). The purpose of our model is not to give a detailed description of the oxidation process trough different stages (O adsorption, island formation, . . .). However, the model allows us to approximately identify the beginning of oxide formation. In this sense, we remark that this picture of the oxidation process is in accord with recent STM mesurements,[4] and our model corresponds well to the forming of an almost complete alumina layer at 1 ML coverage.

ACKNOWLEDGMENTS

M. Alducin and A. Arnau acknowledge partial support from the Spanish DGICYT (Project No. PB97-0636), Eusko Jaurlaritza, Iberdrola S. A., Gipuzkoako Foru Aldundia, and Euskal Herriko Unibertsitatea. S. Peter Apell acknowledges support from the Swedish Natural Science Research Council.

[1] N. Cabrera and N.F. Mott, Rep. Prog. Phys. **12**, 163 (1948).
[2] V. E. Henrich and P. A. Cox, *The Surface Science of Metal Oxides* (Cambridge Press, 1994).
[3] M.V. Finnis, J. Phys.: Condens. Matter **8**, 5811 (1996).
[4] H. Brune, J. Wintterlin, J. Trost, G. Ertl, J. Wiechers, and R.J. Behm, J. Chem. Phys. **99**, 2128 (1993).
[5] J. Jacobsen, B. Hammer, K.W. Jacobsen, and J.K. Nǿrskov, Phys. Rev. B **52**, 14 954 (1995).
[6] J.A. Jensen, C. Yan, and A.C. Kummel, Surf. Sci. **267**, 493 (1995).
[7] L. Österlund, I. Zorić, and B. Kasemo, Phys. Rev. B **55**, 15 452 (1997).
[8] T. Sasaki and T. Ohno, Surf. Sci. **433-35**, 172 (1999).
[9] C.F. McConville, D.L. Seymour, D.P. Woodruff, and S. Bao, Surf. Sci. **188**, 1 (1987).
[10] C. Berg, S. Raaen, and A. Borg, Phys. Rev. B **47**, 13 063 (1993).
[11] R.P. Messmer and D.R. Salahub, Phys. Rev. B **16**, 3415 (1977).
[12] I.P. Batra and L. Kleinmann, J. Electron Spectrosc. Relat. Phenom. **33**, 175 (1984).
[13] J.L. Erskine and R.L. Strong, Phys. Rev. B **25**, 5547 (1982).
[14] S.A. Flodstrom, R.Z. Bachrach, R.S. Bauer, and S.B. Hagström, Phys. Rev. Lett. **37**, 1282 (1976).
[15] R. Martel, Ph. Avouris, and I.W. Lyo, Science **272**, 385 (1996).
[16] H.D. Ebinger and J.T. Yates, Jr., Phys. Rev. B **57**, 1976 (1998).
[17] B.C. Mitrovic and D.J. O'Connor, Surf. Sci. **405**, 261 (1998).
[18] C.J. Powell and J.B. Swan, Phys. Rev. **118**, 640 (1960).

[19] E.A. Stern and R.A. Ferrell, Phys. Rev. **120**, 130 (1960).
[20] R.H. Ritchie, Phys. Rev. **106**, 874 (1957).
[21] A. Borg, P. Apell, and O. Hunderi, Phys. Scr. **35**, 868 (1987).
[22] A. Bagchi, R.G. Barrera, and R. Fuchs, Phys. Rev. B **25**, 7086 (1982).
[23] A.M. Bradshaw, W. Domcke, and L.S. Cederbaum, Phys. Rev. B **16**, 1480 (1977).
[24] D.A. King and M.G. Wells, Surf. Sci. **29**, 454 (1972).
[25] M. Zen, *Atomic and Molecular Beam Methods*, edited by G. Scoles (Oxford University Press, Oxford, 1988), Vol. 1.
[26] D. Pines, *Elementary Excitations in Solids* (Benjamin, New York, 1963).
[27] M. del Castillo-Mussot, R.G. Barrera, T. López-Ríos, and W. Luis Mochán, Solid State Commun. **71**, 157 (1989).
[28] R.G. Barrera and R. Fuchs, Phys. Rev. B **52**, 3256 (1995).
[29] J. Topping, Proc. R. Soc. London Ser. A **114**, 67 (1927).
[30] P.J. Feibelman, Prog. Surf. Sci. **12**, 287 (1982).
[31] A. Liebsch, Phys. Rev. B **36**, 7378 (1987).
[32] A.A. Radzig and B.M. Smirnov, *Reference Data on Atoms, Molecules, and Ions* (Springer-Verlag, Berlin, 1985).
[33] R.H. Ritchie, C.J. Tung, V.E. Anderson, and J.C. Ashley, Radiat. Res. **64**, 181 (1975); C.J. Tung, J.C. Ashley, and R.D. Birkhoff, Phys. Rev. B **16**, 3099 (1977).